Intravascular Coagulation Activation in a Murine Model of Thrombomodulin Deficiency: Effects of Lesion Size, Age, and Hypoxia on Fibrin Deposition

By Aileen M. Healy, Wayne W. Hancock, Patricia D. Christie, Helen B. Rayburn, and Robert D. Rosenberg

We consecutively inactivated both alleles of the thrombomodulin (TM) gene in murine embryonic stem (ES) cells and generated TM-deficient ($TM^{-/-}$) chimeric mice. Quantitation of an ES-cell marker and protein C cofactor activity indicates that up to 50% of pulmonary endothelial cells are ES-cell derived and therefore TM deficient. Infusions of ^{125}I-fibrinogen into mice show a significant increase (fourfold, $P < .005$) in radiolabeled cross-linked fibrin in $TM^{-/-}$ chimeric mouse lung as compared with wild-type mice. However, only chimeric mice that exhibit at least a 30% reduction in protein C cofactor activity and are at least 15 months old display this phenotype. Immunocytochemical localization of TM in chimeras shows a mosaic pattern of expression in both large and small blood vessels. Colocalization of cross-linked fibrin and neo (used to replace TM) reveals that fibrin is deposited in $TM^{-/-}$ regions. However, the fibrin deposits were largely restricted to pulmonary vessels with a lumenal area greater than 100 μm^2. The hypercoagulable phenotype can be induced in younger chimeric mice by exposure to hypoxia, which causes a fivefold increase in β-fibrin levels in lung. Our findings show that TM chimerism results in spontaneous, intravascular fibrin deposition that is dependent on age and the magnitude of the TM deficiency.

THROMBOMODULIN (TM, CD141), the cell-surface receptor for thrombin that suppresses blood coagulation by altering thrombin substrate specificity, converts thrombin from a potent procoagulant (clotting fibrinogen and activating platelets) to an anticoagulant. The TM-thrombin complex cleaves protein C (PC) to activated protein C (aPC), which catalyzes the proteolytic degradation of activated blood clotting factors V and VIII. The physiological role of the TM/PC pathway has been substantiated by data showing that thrombin infusions into animals induces generation of aPC, that humans with defects in this pathway experience an acceleration of thrombin generation, and that a suppression of PC activation commonly precedes a thrombotic episode.[1-3] These observations support the hypothesis that TM plays a critical role in the prevention of thrombus formation.

TM was initially identified as an endothelial cell cofactor[4]; however, subsequent studies documented the presence of TM on synovial cells, meningeal cells, activated smooth muscle cells, macrophages, and platelets.[5-7] In addition to its presence on vascular and nonvascular cells of the adult animal, TM has been localized in the murine embryo as early as gestation day 7.5.[8-11] To investigate the role that TM plays in regulating blood coagulation in adult mice, as well as the function of TM during murine embryogenesis, we performed gene targeting studies in murine embryonic stem (ES) cells to generate mice heterozygous or homozygous for the TM deletion. We previously reported that embryos homozygous for the TM deletion die in utero by embryonic day 9.5.[12] The TM-null phenotype thus precluded further investigations into the effects of TM homozygous deficiency on coagulation function in adult mice. As one approach to bypass the embryonic lethal phenotype of TM-null mice, we generated homozygous TM-null ES cells to produce TM-deficient ($TM^{-/-}$) chimeric mice.

In the present study, we examined the effects of a TM deficiency in adult mice. The data show that $TM^{-/-}$ chimeric mice have reduced PC cofactor activity as compared with wild-type mice, and exhibit an age-dependent increase in urea- and acid-insoluble intravascular fibrin. Cross-linked fibrin was detected in the pulmonary vasculature in regions of the vessel wall deficient in TM and fibrin deposition was largely dependent on the size of the $TM^{-/-}$ region. Furthermore, the heightened procoagulant phenotype of $TM^{-/-}$ chimeric mice could be reproduced in an age-independent manner by challenging animals with hypoxia. These results indicate that TM is a necessary component of the anticoagulant mechanism for the prevention of thrombosis, and are consistent with the hypothesis that a TM deficiency is a quantitative trait like hypertension.

MATERIALS AND METHODS

Generation of $TM^{-/-}$ ES cells and chimeric mice. We used a single targeting construct to create TM double-deletion mutants ($TM^{-/-}$). Briefly, $TM^{+/-}$ ES cells previously generated using the positive/negative drug selection strategy[12,13] were reselected with the positive selecting agent, geneticin (G418; GIBCO-BRL, Rockville, MD), as described.[14] $TM^{+/-}$ ES cells were grown for 2 weeks in complete media supplemented with 2.0 mg/mL geneticin and every other day during drug reselection, washed with phosphate-buffered saline, and refed in complete media supplemented with geneticin. DNA was isolated from surviving clones and analyzed by the Southern blot technique and by polymerase chain reaction to identify the TM-null ES cells. In vitro differentiation of ES cells was performed as previously described.[15] Embryoid bodies were scored on day 4 of differentiation for the formation of cystic structures and again on days 7 and 10 for the presence of blood islands and contracting myocytes. The $TM^{-/-}$ ES cells were injected into the blastocoel of 3.5-day C57BL/6 embryos, reimplanted into pseudopregnant recipients, and carried to term. The resulting offspring were maintained for analysis of a hypercoagulable phenotype.

From The Pulmonary Center, Boston University School of Medicine; the Department of Pathology, Harvard Medical School, Boston, MA; and the Department of Biology, Massachusetts Institute of Technology, Cambridge, MA.

Submitted June 17, 1998; accepted August 4, 1998.

Supported by National Institutes of Health Grants No. RO1 HL53396, PO1 41484 (R.D.R.), and RO1 HL60579 (W.W.H.). A.M.H. was the recipient of an American Heart Association Fellowship Award from the Massachusetts Affiliate.

Address reprint requests to Aileen M. Healy, PhD, The Pulmonary Center, Boston University School of Medicine, 80 E Concord St, Boston, MA 02118; e-mail: ahealy@bupula.bu.edu.

The publication costs of this article were defrayed in part by page charge payment. This article must therefore be hereby marked "advertisement" in accordance with 18 U.S.C. section 1734 solely to indicate this fact.

0006-4971/98/9211-0017$3.00/0

Preparation of ^{125}I-labeled murine fibrinogen. Fibrinogen was isolated from the platelet-poor plasma of C57BL/6 mice by two successive precipitations with 25% saturated ammonium sulfate.[16] Murine fibrinogen was radiolabeled with Na^{125}I (Amersham, Arlington Heights, IL) to a specific activity of approximately 1.0 μCi NaI/μg of fibrinogen using Iodogen beads (Pierce, Rockford, IL). For radiolabeling, a 200 μg/250 μL solution (2.2 μmol/L) of fibrinogen in 0.15 mol/L NaCl, 0.02 mol/L Tris-HCl, pH 7.4, was incubated with two Iodogen beads and 1.0 mCi Na^{125}I (17.4 mCi ^{125}I/μg of iodine) for 2.5 minutes at room temperature. Radiolabeled fibrinogen was separated from free NaI by chromatography on a 0.5 × 12.5–cm G-75 Sephadex column (Sigma, St Louis, MO). Autoradiography of the ^{125}I-fibrinogen following sodium dodecyl sulfate (SDS) polyacrylamide gel electrophoresis under reducing or nonreducing conditions showed that murine fibrinogen was the major radiolabeled protein, with no significant contaminating proteins.

Quantitation of ^{125}I-labeled fibrin deposition in mice. TM wild-type mice and TM$^{-/-}$ chimeric mice received 0.5 μCi of ^{125}I-labeled fibrinogen by injection into the lateral tail vein on days 1, 3, and 5, and the organs were collected for analysis on day 7 (the half-life of circulating ^{125}I-fibrinogen is approximately 9 to 12 hours). Forty-eight hours after the final injection, animals received 0.2 mL of an anticoagulant solution containing 2.4 mg/mL heparin (80 *United States Pharmacopeia* units), 10 mg/mL ϵ-amino-n-caproic acid, and 0.05 μg/mL (42 U/mL) aprotinin (Sigma) in 0.15 mol/L NaCl. Mice were lightly anesthetized with ether and killed by cardiac puncture, at which time 1.0 mL of whole blood was collected for isolation of platelet-poor plasma. Circulating ^{125}I-fibrinogen (cpm/μL) was determined for an aliquot of plasma, and organs were dissected and tissue fragments prepared for several analyses. First, organs or organ fragments were snap frozen in liquid nitrogen for later analysis of PC activity and glycerol phosphate isoenzymes. Second, organs were embedded in OCT compound (Miles Laboratories, Eckhardt, IN) and frozen in an isopentene bath cooled with dry ice for analysis by immunohistochemistry. Third, tissue samples were weighed, homogenized in extraction buffer (0.01 mol/L Na-phosphate, pH 7.5; 10 U/mL heparin; 2 mg/mL EDTA; 10 U/mL aprotinin; and 0.1 mmol/L phenylmethylsulfonyl fluoride [PMSF]) and prepared for extraction of ^{125}I-fibrinogen and fibrin as described.[17] Homogenates were extracted at 4°C for 18 hours, centrifuged at 1,000*g* for 20 minutes, the supernatants removed, and the pellets washed once in 0.5 mL of extraction buffer. The supernatant was again removed and pooled with the previous supernatant. Similarly, both pellets were combined, resuspended in 1.5 mL of freshly prepared 3 mol/L urea, extracted at 37°C for 2 hours with rotation, and then centrifuged at 1,000*g* for 20 minutes. The urea-soluble cpm in the supernatants and the urea-insoluble cpm in the pellets were quantified in a gamma counter (LKB 1272 clinigamma, Uppsala, Sweden).

Determination of glycerol phosphate isoenzyme and TM cofactor activity in TM$^{-/-}$ chimeric mice. The contribution of TM$^{-/-}$ ES cells to chimeric mice was assessed using three criteria; the first was an estimation of the agouti coat color. The TM-null ES cells were derived from the 129 mouse, which expresses the agouti or brown coat color, and the recipient embryo is derived from the C57BL/6 mouse, which expresses a black coat color. The resulting chimeric offspring show a combination of agouti and black coat coloring; the more agouti coloring, the greater the ES-cell contribution to the mouse. The second criteria was the differential electrophoretic mobility of glycerol phosphate isoenzymes, which is an indication of cell contribution to whole organs.[18] The isoforms of glycerol phosphate were electrophoretically separated on cellulose acetate, detected by staining for enzyme activity and the relative contribution of each isoenzyme and therefore each genotype, quantified by densitometry. Third, the contribution of TM-null ES cells to endothelial cells was determined using the TM-dependent activation of PC by thrombin. Sections of mouse lung that had been frozen in liquid nitrogen immediately after dissection were pulverized with a mortar and pestle while still frozen. Tissue fragments were extracted in 0.3 mL of lysis buffer (2% Triton X-100, Sigma; 0.01 mol/L Tris-HCl, pH 8.1; 10 mg/mL pepstatin; 10 mg/mL leupeptin; 0.1 mmol/L PMSF; and 0.02% NaN_3) at 4°C for 30 minutes with rotation. Extracts were then clarified by centrifugation at 16,000*g* at 4°C for 15 minutes. The protein concentration of the supernatants was determined by Bradford assay. For cofactor determination, 0.05 μmol/L human PC, and 0.05 μmol/L human thrombin (Enzyme Research Labs, South Bend, IN) plus 0.5 μg of lung extract was incubated in 0.15 mol/L NaCl; 0.02 mol/L Tris-HCl, pH 7.4; 2.5 mmol/L $CaCl_2$; and 5 mg/mL bovine serum albumin at 37°C for 15 minutes. Human antithrombin III (Enzyme Research Labs) and hirudin (Sigma) were then added to stop the reaction and aPC was measured using the colorimetric reagent, S2236 (Pharmacia, Piscataway, NJ).

Histology and immunocytochemistry. Organs (lung, heart, liver, kidney, and spleen) collected from wild-type and chimeric mice were fixed in formalin or snap frozen and stored at −70°C. Formalin-fixed tissues were embedded in paraffin, sectioned, and stained with hematoxylin and eosin (H&E). Cryostat sections obtained from snap-frozen tissues were used for the localization of TM and neomycin phosphotransferase (neo, the product of the bacterial gene used to replace the TM coding region). To identify intravascular cross-linked fibrin, acid-insoluble fibrin was also localized in cryosections.

For TM and neo localization, serial sections (4 μ) fixed in paraformaldehyde-lysine-periodate (PLP) were incubated overnight at 4°C with a rat anti-mouse TM monoclonal antibody (MoAb; gift of Dr Stephen Kennel, Oak Ridge Labs, Oak Ridge, TN) and a rabbit anti-neo antibody (5 Prime 3; Prime Inc, Boulder, CO). To localize acid-insoluble fibrin, cryostat sections were acid washed with 2% acetic acid in neutral-buffered formalin at room temperature for 20 minutes,[19] followed by incubation with a rabbit antibody recognizing fibrinogen and fibrin (Dako, Carpinteria, CA). Sections were washed and bound primary antibodies were detected by successive incubations with bridging antibodies, rabbit peroxidase-antiperoxidase complexes (Dako), the substrate, diaminobenzidine, and finally counterstained with hematoxylin.[20] Specificity controls included the use of isotype-matched rat MoAbs or normal rabbit immunoglobulin in place of specific primary antibodies: endogenous peroxidase was blocked using methanol containing 0.03% hydrogen peroxide.[20]

Morphometry. Sequential tissue sections (4 μ) stained for H&E, neo, and cross-linked fibrin were analyzed using the Bio-Quant Imaging System (R&M Biometrics, Nashville, TN). Four to six sequential sections were cut for each staining condition and a single section from each condition was chosen as suitable to measure blood vessel lumenal area. Three nonoverlapping fields (20× objective) and two nonoverlapping fields (60× objective) were selected from each section, and each chosen field from a section corresponded to the same field of the sequential sections. Lumenal areas were traced from digitized images of 175,000 μm^2 (20× objective) or 20,000 μm^2 (60× objective).

Exposure of TM$^{-/-}$ chimeric mice to hypoxia. TM$^{-/-}$ chimeric mice, aged 6 to 11 months, were exposed to hypoxic conditions by placing animals in a purge box (Innovative Systems, Inc, Newton, MA) to achieve a final oxygen content of 8% for 16 to 18 hours. Animals maintained in room air were used as normoxic controls. After exposure to normoxic or hypoxic conditions, mice received a lethal, intraperitoneal injection of anesthesia, followed by an intravenous injection containing 300 to 450 U of heparin via the lateral tail vein. Whole lung was dissected and snap frozen in liquid nitrogen.

Cross-linked fibrin was extracted from lung homogenates as described above (see quantitation of ^{125}I-labeled fibrin). The final tissue pellet is solubilized in SDS-sample buffer containing 5% 2-mercaptoethanol, incubated at 65°C for 90 minutes, electrophoresed on a 7.5% polyacrylamide gel, and transferred to PVDF nylon membrane (Millipore, Bedford, MA) for Western blot analysis of β-fibrin. β-fibrin was detected using an MoAb against the N-terminus of the Bβ-fibrin chain

(MoAb 59D8; gift of Dr Marshall Runge, Galveston, TX) and enhanced chemiluminescence (ECL; Amersham).

RESULTS

TM gene inactivation in ES cells and generation of TM$^{-/-}$ chimeras. We produced an ES-cell clone containing a homozygous deletion of the TM gene. The resulting clone contained the neo gene in place of the TM coding region, thereby creating a double knockout or homozygous TM-deletion mutant. The homozygous TM gene deletion is shown by Southern blot analysis (Fig 1). The results shown in Fig 1, lane 3 demonstrate that the 10-kb *Bgl*II or wild-type TM gene fragment is absent in TM$^{-/-}$ ES cells, and confirms the presence of a single 3.3-kb band, which results from the introduction of a novel *Bgl*II restriction enzyme site contributed by the neo sequences. TM$^{-/-}$ ES cells were analyzed by Southern blotting using three different probes corresponding to DNA sequences both internal to and external to the inactivated locus and all three probes demonstrate the predicted pattern (not shown). In addition, TM$^{-/-}$ ES cells contain a normal karyotype.

The prolonged growth of ES cells in culture diminishes the pluripotency of the stem cells and thus the ability to contribute uniformly to cellular lineages during embryonic differentiation.[18] We tested TM$^{-/-}$ ES-cell pluripotency by in vitro and in vivo differentiation.[15,21] ES-cell differentiation under nonadherent culture conditions results in the formation of cystic structures called embryoid bodies, which display specific developmental markers. Hemoglobin-containing blood islands appear after 7 days of suspension culture and clusters of contracting cells are present after 10 days in culture. These structures represent the differentiation of hematopoietic and endothelial cells as well as cardiomyocytes. ES cells were grown in suspension culture for 4, 7, or 11 days and scored for the presence of cystic structures on day 4, acetylated–low density lipoprotein (LDL) uptake on day 7, and contracting cells on day 11.[22] Between 39 and 100 embryoid bodies were counted for each condition in duplicate. There were no significant differences in the number of cystic structures, embryoid bodies staining positive for acetylated-LDL uptake, or contracting muscle among all three genotypes. These results suggest that TM$^{-/-}$ ES cells differentiate in vitro at the same frequency as controls. The presence of all three of these characteristic differentiation markers in TM$^{-/-}$ ES cells suggests that the prolonged culture conditions required to delete the second TM allele did not adversely affect ES-cell differentiation in vitro. TM$^{-/-}$ ES-cell pluripotency was shown in vivo by generating ES-cell–derived chimeric mice.

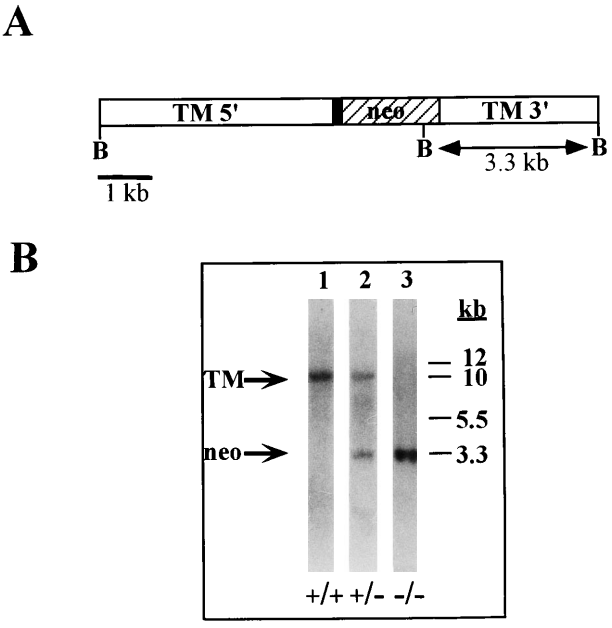

Fig 1. Illustration of targeted TM locus and Southern blot of TM-null ES cells. (A) Diagram of the targeted TM gene indicating the 5′ upstream region of the TM promoter (TM 5′), 153 bp of untranslated TM sequences (■), the neo expression cassette used to replace the TM coding region (neo, ▨), and 3′ TM untranslated sequences (TM 3′). *Bgl*II restriction enzyme sites are indicated at B. (B) Southern blot analysis of ES-cell genomic DNA. Genomic DNA was isolated from wild-type ES cells (lane 1), from TM$^{+/-}$ ES cells (lane 2) and from TM$^{-/-}$ ES cells (lane 3) and hydrolyzed with *Bgl*II restriction enzyme. The hydrolyzed DNA was electrophoresed, blotted, and hybridized with a ^{32}P-labeled cDNA probe against DNA sequences within the TM 3′ region. Markers are indicated in kb.

The resulting chimeric offspring (129 ES cells on a C57BL/6 background) were initially categorized by the degree of agouti coat coloring, which ranged from 20% to 80%. The agouti locus and the TM gene are both located on chromosome 2 in the mouse; therefore, the agouti coat coloring is an approximation of TM chimerism.[23] For analysis of the TM-deficiency, the animals were separated into two groups: high-percentage chimeras (50% to 80% agouti coat coloring) or low-percentage chimeras (20% to 50% agouti coat coloring). All TM$^{-/-}$ chimeras appear healthy and normal in size and weight. Routine histological analyses of TM$^{-/-}$ chimeras from 2 months to 2 years of age show no genotype-specific pathologies in any of the tissues examined or within the lumen of blood vessels where TM is widely expressed.

Age-related increase in urea-insoluble fibrin in TM$^{-/-}$ chimeric mice. To investigate the effects of a TM deficiency on the coagulation system, we examined TM$^{-/-}$ chimeric mice for the spontaneous deposition of ^{125}I-labeled fibrin in heart, lung, liver, spleen, and kidney. Whole organ homogenates were extracted in urea, which results in two fractions. The first fraction is composed of urea-soluble cpm that contain ^{125}I-fibrinogen, soluble fibrin, and fibrin degradation products, and the second fraction is composed of urea-insoluble cpm that contain cross-linked ^{125}I-fibrin and fibrin degradation products (A.M.H. and R.D.R., unpublished observations, November 1994).[17] The high-percentage chimeras have up to a fivefold increase in urea-insoluble cpm in lung ($P < .005$) and a twofold increase in urea-insoluble cpm in liver ($P < .01$) as compared with age-matched, wild-type mice and low-percentage chimeras (Fig 2, top). No difference is observed in urea-insoluble cpm in heart, kidney, or spleen (results not shown). This increase in urea-insoluble cpm is age dependent; animals attaining 15 to 20 months are affected, whereas animals 6 to 11 months remain unaffected (Fig 2, bottom). These results suggest that an age-related, prothrombotic phenotype develops spontaneously in the lungs and liver of TM$^{-/-}$ chimeric mice.

Contribution of TM$^{-/-}$ ES cells to chimeric mice. The marked increase of urea-insoluble ^{125}I-fibrin in the TM$^{-/-}$

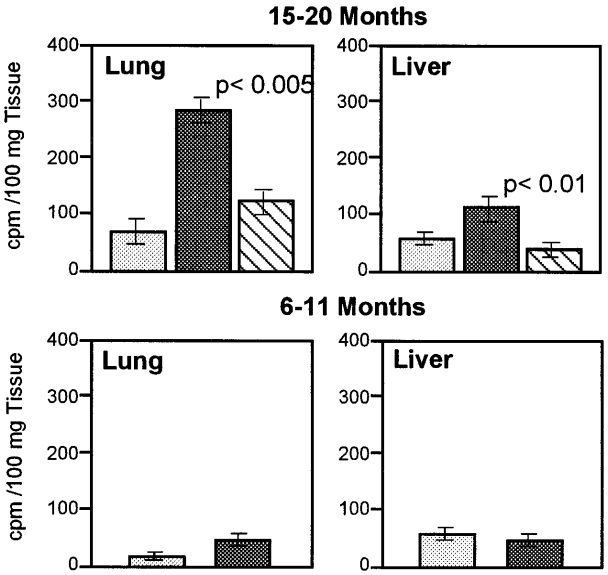

Fig 2. Quantitation of ^{125}I-labeled cross-linked fibrin in TM$^{-/-}$ chimeric and wild-type mice. ^{125}I-labeled fibrinogen was intravenously infused into mice and urea-insoluble extracts were prepared. ^{125}I-labeled urea-insoluble counts were quantitated and the cpm from five or six animals from each genotype was averaged. Cross-linked fibrin from lung and liver of 15- to 20-month-old mice (top) and 6- to 11-month-old mice (bottom) is shown. (▭), TM$^{+/+}$; (▬), high-percentage chimeras; (▨), low-percentage chimeras.

chimeric mouse lung led us to analyze the contribution of TM$^{-/-}$ ES cells to lung tissue. We used the differential expression of the glycerol phosphate isoenzymes (GPI): the ES cell is homozygous for the ''type a'' isoenzyme whereas the C57BL/6 host is homozygous for the ''type b'' isoenzyme.[18] The percentage of GPIa detected in whole lung lysates is shown in Table 1. The GPIa average value for the high-percentage chimeras is 33% (range, 26% to 40%) and the GPIa average value for the low-percentage chimeras is 20% (range, 18% to 23%). These results indicate the percentage of chimeric lung that is ES-cell derived. However, these values represent the ES-cell contribution to all cell types in the lung, not just the endothelium.

To assess the TM$^{-/-}$ ES-cell contribution to the endothelium, TM cofactor activity was measured in these same lung extracts. The average TM cofactor activity for the high-percentage chimeras is 14 ng aPC/minute compared with 20 ng aPC/minute in wild-type mice. This represents a 31% reduction from wild-type levels. The average TM cofactor activity for the low-percentage chimeras is 17 ng aPC/minute or a 17% reduction from wild-type levels. These values correspond closely to the values obtained with the GPI assay for TM$^{-/-}$ ES-cell contribution to lung and indicate that, on average, from 17% to 31% of the endothelium in TM$^{-/-}$ chimeric mice do not express TM.

Table 1. ES-Cell Contribution to TM Chimeric Mice

	GPI	APC
High-percentage chimeras (n = 5)	33% (range, 26% to 40%)	14 ng/minute (3)*
Low-percentage chimeras (n = 5)	20% (range, 18% to 23%)	17 ng/minute (3)

Lung lysates prepared from TM$^{-/-}$ chimeric mice were used to identify GPI by cellulose acetate gel electrophoresis and staining for GPI activity. The percentage of each isozyme was determined from digitized images of the cellulose acetate gels. Using the same lung tissue from each mouse the APC was determined.

Abbreviation: APC, PC cofactor activity.

*The standard deviation for the APC measurement is shown in parentheses.

TM expression in chimeric lung. TM is expressed at the lumenal surface of virtually all vascular endothelium.[6,24,25] This is shown in the murine lung using immunocytochemistry to examine tissue sections from wild-type animals, where we found all pulmonary endothelial cells stain positive for TM (Fig 3a). TM immunolocalization provides a means to distinguish TM-expressing and nonexpressing endothelium, thereby identifying those endothelial cells presumably derived from TM-null ES cells. When we examined the pulmonary endothelium of TM$^{-/-}$ chimeric mice, we found TM localized in a mosaic pattern. Cross sections through single vessels showed an intact endothelium with examples of either all endothelial cells staining positive for TM (Fig 3b), endothelial cells staining positive adjacent to endothelial cells negative for TM (Fig 3c), or endothelial surfaces entirely negative for TM staining (Fig 3d). A similar TM expression pattern was observed in the vasculature of liver and kidney in TM$^{-/-}$ chimeric mice regardless of age (not shown). The mosaic expression pattern in TM$^{-/-}$ chimeric mice is not restricted to a subset of vessels; mosaicism is observed in large- and small-caliber vessels in both the arterial and venous vasculature.

Immunolocalization of cross-linked fibrin and neo in chimeric mouse lung. To map the intravascular fibrin deposits that were initially identified by quantitating urea-insoluble ^{125}I-labeled fibrin (Fig 2), we immunolocalized acid-insoluble fibrin in murine lung.[19] Only focal and low-level fibrin deposition was detected in lung sections from wild-type mice (Fig 4a), which was in contrast to the intense fibrin labeling in corresponding sections from TM$^{-/-}$ chimeric mice (Fig 4b). In general, the most remarkable fibrin localization occurred in small muscular arteries, although fibrin deposition was also evident in large and small veins. The localization of acid-insoluble fibrin in the 6- to 11-month-old TM$^{-/-}$ chimeric mice was comparable with that observed for wild-type mice (not shown).

We next determined whether fibrin is deposited on those regions of the intimal surface deficient in TM. As stated, the neo gene is expressed in endothelial cells derived from TM$^{-/-}$ ES cells. Therefore, endothelial cells immunoreactive with anti-neo antibodies lack TM. Colocalization studies in serial sections showed that pulmonary blood vessels of TM$^{-/-}$ chimeric mice which displayed labeling for acid-insoluble fibrin (Fig 5, arrows) were also immunoreactive for neo (Fig 5, arrows), whereas sites lacking fibrin deposition were correspondingly deficient in neo expression (Fig 5, asterisk).

Although we could colocalize neo and fibrin in sequential sections of a single vessel, we observed that fibrin localization was not present in all neo-positive vessels and was almost completely absent from the microvasculature. To determine whether we could further classify the types of vessels showing fibrin deposition, we measured the lumenal areas of all blood

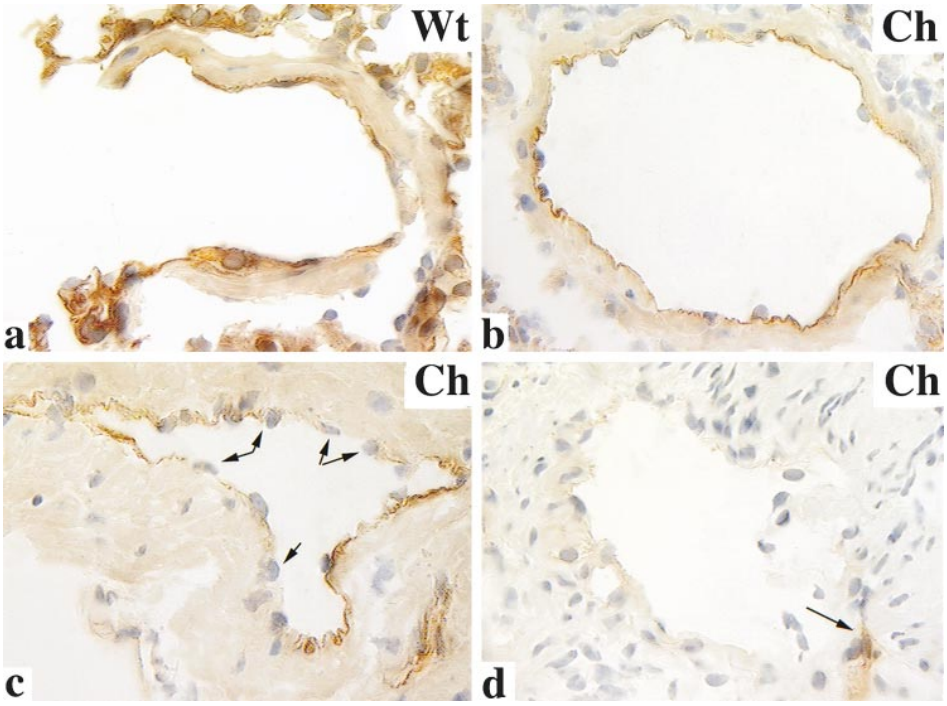

Fig 3. TM immunolocalization in wild-type (Wt) and TM$^{-/-}$ chimeric (Ch) lung. PLP-fixed cryosections of mouse lung were stained with an anti-TM rat MoAb and counterstained with hematoxylin. TM is localized to the intimal surface of wild-type mice (a) and some TM$^{-/-}$ chimeric vessels (b). TM mosaicism is shown in cross sections through blood vessels containing patchy TM staining (c); arrows indicate endothelial nuclei confirming the presence of an intact intima. Also observed are blood vessels completely negative for TM localization (d); arrow indicates adjacent blood vessel immunoreactive with anti-TM antibodies. Original magnification × 630.

vessels present within an H&E-stained lung section as compared with the lumenal areas of blood vessels that stained positive for neo and fibrin. The morphometric analysis of sequential lung sections showed that neo-positive (ie, TM$^{-/-}$) vessels displayed a similar frequency distribution as the H&E-stained sections (Table 2): 88% of total blood vessels and 71% of neo-positive blood vessels have a lumenal area less than 100 μm^2. This is in contrast to the frequency distribution of the cross-linked, fibrin-stained vessels, because only 15% of fibrin-stained vessels have a lumenal area less than 100 μm^2. Although the possibility exists that the absence of cross-linked fibrin in the microvasculature results from a fixation artifact, we found that the localization of acid-insoluble fibrin in another TM$^{-/-}$ mouse, the TM$^{Pro/Pro}$ mouse, showed the presence of cross-linked fibrin deposited throughout the pulmonary vasculature in both microvessels and in larger caliber vessels.[26] Collectively, the results of the immunocytochemical and morphometric analyses suggest that fibrin deposition is a single-vessel effect controlled not only by the extent of the TM deficiency but also by vessel size and type.

Fibrin deposition in response to hypoxia. The results of the ^{125}I-labeled fibrin analysis in the 6- to 11-month-old TM$^{-/-}$ chimeric mice (Fig 2) suggest that an increased thrombotic potential exists in these animals but is manifested only in response to a second stimulus such as increased age or environmental factors. To test this hypothesis, we measured the endogenous β-fibrin levels in 6- to 11-month-old TM$^{-/-}$ chimeric mice either exposed to hypoxia (8% O_2) or maintained at normoxia (21% O_2). The data obtained from pairing TM$^{-/-}$ chimeric mice by agouti coat coloring and challenging one animal from each pair with hypoxia are shown in Fig 6. These data show that exposure of TM$^{-/-}$ chimeric mice to hypoxia results in a fourfold increase in cross-linked β-fibrin in lung over paired controls ($P < .005$). Wild-type mice exposed to hypoxia show a similar fourfold increase in cross-linked β-fibrin in lung compared with normoxic control mice. However, the ambient levels of β-fibrin are sixfold higher in the TM$^{-/-}$ chimeras as compared with wild-type mice (ie, 0.11 μg fibrin/.1 g tissue *v* 0.50 μg fibrin/.1 g tissue in wild-type mice under normoxic versus hypoxic conditions, respectively, and 0.62 μg fibrin/.1 g tissue *v* 2.64 μg fibrin/.1 g tissue in TM$^{-/-}$ chimeras).

DISCUSSION

Mutations in the TM/PC anticoagulant pathway are quite common in humans. Alterations in PC function are often associated with an increased risk of thrombosis, although many affected individuals remain free of thrombotic complications.[27] Conversely, if a population of patients displaying thrombotic complications are identified with heterozygous deficiencies in the TM/PC pathway, the occurrence of a thrombotic phenotype in these patients is 10 to 25 times higher than in the general population. These findings suggest that an inherited predisposition to thrombosis may result from an additional mutation in the anticoagulant pathways. It has long been postulated that a variant TM gene could be the second genetic defect precipitating a thrombotic episode. This hypothesis has gone largely untested because the endothelium is not readily sampled to test for such defects.[28] Therefore, we generated a murine model for TM deficiency to directly test how alterations in TM function contribute to the pathogenesis of thrombosis.

We replaced both alleles of the TM gene with the neo gene in ES cells and used these homozygous mutant ES cells to generate chimeric mice showing distinct TM deficiencies. We analyzed TM$^{-/-}$ chimeric mice for the presence of a thrombotic propensity by quantitating urea-insoluble ^{125}I-fibrin extracted from organs of mice infused with ^{125}I-fibrinogen and by the immunolocalization of acid-insoluble fibrin in these same

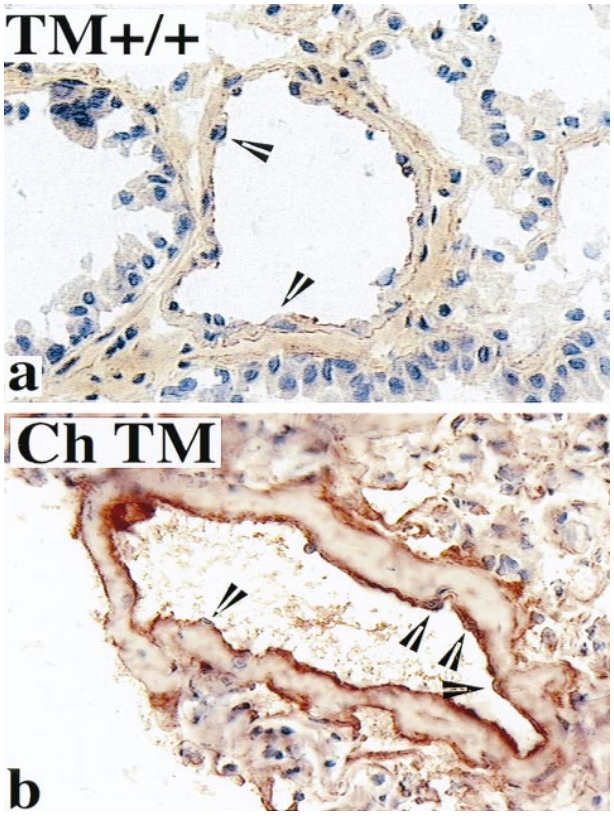

Fig 4. Localization of acid-washed fibrin/fibrinogen in the murine pulmonary vasculature. PLP-fixed cryosections of mouse lung were acid washed to solubilize fibrinogen and fibrin degradation products before immunolocalization with an anti-fibrin/fibrinogen IgG and counterstaining with hematoxylin. Wild-type ($TM^{+/+}$) mice between 15 and 20 months of age display little or no immunoreactivity at the intimal surface (representative image shown in a), whereas age-matched $TM^{-/-}$ chimeric (Ch TM) mice display a strong cross-linked fibrin immunolocalization at the lumenal surface of blood vessels (b). Endothelial cell nuclei are indicated by arrowheads. Original magnification × 400.

Table 2. Comparison of Total Blood Vessels With Neo-Stained and Cross-Linked, Fibrin-Stained Pulmonary Blood Vessels

Lumenal Area (μm^2)	Frequency (*f*)			Cumulative Relative *f* (%)		
	Total	Neo	FB	Total	Neo	FB
1-10	84	18	1	22	14	5
11-50	195	50	1	74	53	10
51-100	51	22	1	88	71	15
101-250	26	16	8	94	84	55
251-500	10	12	3	97	93	70
501-1,000	8	5	4	99	98	90
1,001-1,500	3	3	2	100	100	100
n	377	126	20			

Sequential lung sections were stained for H&E, neo- or cross-linked fibrin, and the lumenal area of positive vessels was traced electronically. The distribution of positive vessels from six microscope fields per condition is displayed as the frequency and the percent cumulative frequency. The correlation coefficient = 0.986 for the neo-positive vessels and corresponding H&E-stained vessels from a single microscope field of two sequential sections.

organs. The amount of insoluble or cross-linked fibrin corresponds to ES-cell contribution to whole lung, as measured by the isoenzymes of glycerol phosphate and the thrombin-dependent activation of PC. We found that the chimeric mice containing the highest contribution from the TM-null ES cells (ie, high-percentage chimeras containing up to a 40% relative contribution from ES cells, shown in Table 1) are those animals expressing both the lowest TM levels and a significant increase in ^{125}I-labeled, urea-insoluble fibrin. This thrombotic phenotype is age dependent: high-percentage chimeras between 15 and 20 months show a significant increase in urea-insoluble fibrin in lung and liver. The high-percentage chimeras between 6 and 11 months have not yet developed this phenotype, whereas wild-type mice and low-percentage TM chimeras do not show increased urea-insoluble ^{125}I-fibrin, regardless of age. These results are consistent with spontaneous intravascular fibrin formation in $TM^{-/-}$ mice and suggest that over a prolonged

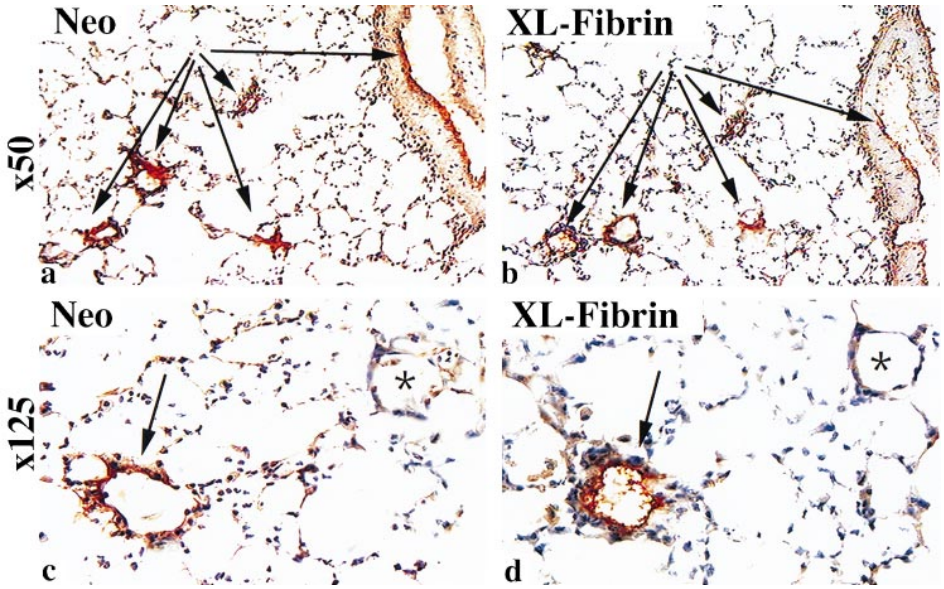

Fig 5. Colocalization of cross-linked fibrin and neo in $TM^{-/-}$ chimeric mouse lung. PLP-fixed cryosections of mouse lung were stained with anti-neo antibody and acid-washed serial sections stained with the anti-fibrin/fibrinogen antibody before counterstaining with hematoxylin. Shown is a representative image from a high-percentage chimeric mouse in the 15- to 20-month age group. Low-power views of serial cross sections show that neo (a) is present in the same blood vessels that demonstrate immunoreactivity for cross-linked fibrin (XL-Fibrin, b). Higher power magnification, c and d, of the same images as shown in a and b. Arrows indicate blood vessels. Original magnification in panels a and b, × 50; panels c and d, × 125.

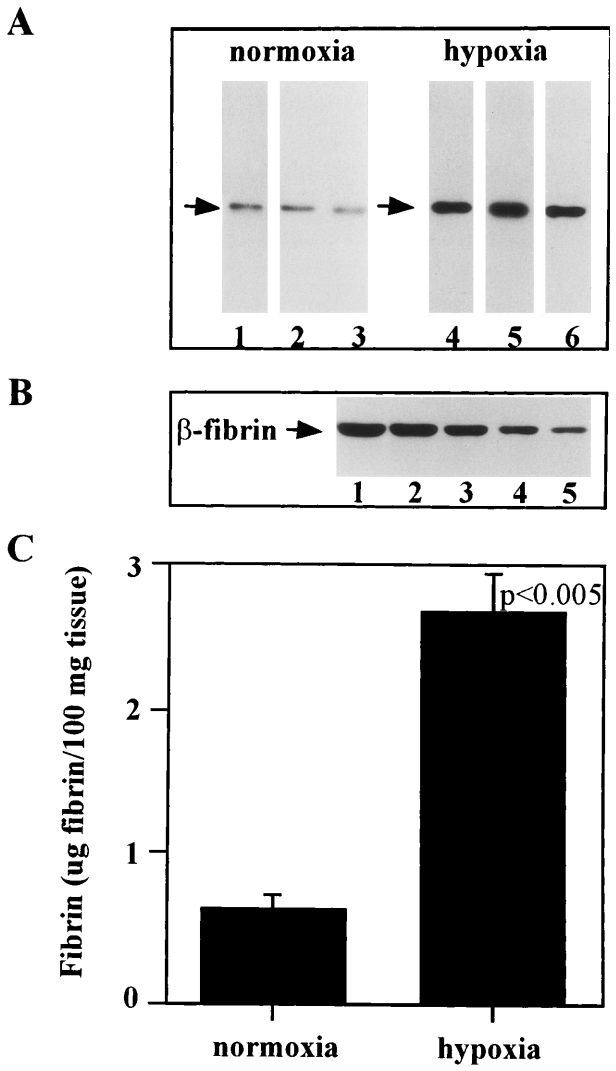

Fig 6. Hypoxia induces fibrin deposition in $TM^{-/-}$ chimeric mice. (A) Western blot of β-fibrin from 6- to 11-month-old TM chimeras. Mice were paired according to agouti coat coloring and one animal from each pair was maintained under normoxic conditions (lanes 1, 2, and 3) while the other was exposed to hypoxic conditions (lanes 4, 5, and 6). Western blot analysis of urea-insoluble tissue samples was conducted using an MoAb against the amino-terminus of Bβ-fibrin. (B) Western blot of purified β-fibrin showing the standard curve containing: lane 1, 250 ng; lane 2, 150 ng; lane 3, 100 ng; lane 4, 50 ng; and lane 5, 20 ng. (C) Quantitation of cross-linked fibrin from Western blot shown in A. Values are expressed as μg β-fibrin per 100 mg of lung tissue.

time period a TM deficiency alters the hemostatic mechanism in favor of the procoagulant response.

The results of our investigation reveal several factors that contribute to the development of a prothrombotic phenotype and provide insight into the physical characteristics of vascular lesion formation. Our most surprising finding is that the actual physical size of the $TM^{-/-}$ area or procoagulant foci limits fibrin formation and deposition. With few exceptions, it is those $TM^{-/-}$ vessels showing a lumenal area in excess of 100 μm^2 that also show cross-linked fibrin deposition. Moreover, these focal gaps in anticoagulant function are autonomous of hemostatic function in general because animals with the highest TM deficiency show no manifestation of thrombotic disease other than these localized, intravascular fibrin deposits. Using chimeric technology, we can now test whether this single-vessel, quantitative trait is also generated from other mutations in the coagulation mechanism.

Our results indicate that coagulation activation and thrombin generation occur normally in mice and that TM functions to counter the procoagulant effects of thrombin. As stated, the increased urea-insoluble ^{125}I-fibrin observed in $TM^{-/-}$ chimeric mice results from focal gaps in TM expression. However, the morphometric analysis of sequential lung sections localizing cross-linked fibrin as compared with neo shows that fibrin deposits are disproportionately absent from the $TM^{-/-}$ microvessels. Although the mechanism remains unclear, one possibility is that the TM pathway (ie, either TM and/or aPC) functioning on wild-type endothelium may be sufficient to neutralize thrombin generated at the lumenal surface of neighboring $TM^{-/-}$ cells and this ability is lost when the distance between TM-expressing and nonexpressing cells becomes too great. Whether fibrin deposition is the direct result of decreased TM or the presumed decrease in aPC generation remains unknown, in part because of the difficulty in quantifying local aPC. Alternatively, the other natural anticoagulant pathways (ie, the heparin-antithrombin III mechanism, the vasoactive substances prostacyclin and nitric oxide, and the fibrinolytic mechanism) may compensate for the loss of TM function, thereby preventing fibrin deposits in small $TM^{-/-}$ regions.

A similar compensatory effect is observed when urea-insoluble ^{125}I-fibrin levels are compared between the high- and low-percentage chimeras. The increased urea-insoluble ^{125}I-fibrin observed only in the high-percentage chimeras suggests that a threshold exists for TM anticoagulant function. Chimeric mice showing reductions from wild-type TM levels of approximately 24% or more display an increased and localized cross-linked fibrin, whereas mice showing reductions less than 24% remain unaffected, even though these levels are decreased from wild-type TM levels. This observation further supports the supposition that either the TM/PC pathway functioning in wild-type endothelial cells or the other natural anticoagulant pathways complement $TM^{-/-}$ regions. The phenotype observed in $TM^{-/-}$ chimeric mice may be analogous to the results obtained with intravenous infusions into mice of neutralizing anti-TM antibody, which blocks cell-surface–associated TM activity in vivo and enhances the likelihood of a lethal thrombotic event after injection of thrombin into the tail vein.[29] Collectively, these results suggest that thrombosis is a quantitative trait, ie, the development of a thrombotic phenotype is correlated with the magnitude of the reduction in TM functional levels.

A second contributing factor to the prothrombotic phenotype is organ-specific variations in endothelial cell hemostatic function. The evidence emerging from studies in transgenic and knockout mice suggests that the coagulation mechanism is controlled by the local microenvironment present in different organs and tissues.[30,31] Hemodynamic forces, cell-cell interactions, soluble factors, and tissue-specific gene expression all contribute to locally regulated hemostasis.

Indeed, comparison of the $TM^{-/-}$ chimeric mouse with another TM-mutant mouse, the $TM^{Pro/Pro}$ mouse, shows distinct qualitative and quantitative differences in their respective hemostatic function. In our previous investigation[26] we characterized the thrombotic phenotype of the $TM^{Pro/Pro}$ mice, which carry a single targeted mutation in the TM coding region that corresponds to a Glu to Pro substitution at position 387 in the human gene. This point mutation results in expression of the intact TM receptor in vivo, but PC activation is reduced by 95%. Therefore, the $TM^{-/-}$ chimeric mice display a more subtle mutation (PC activation reduced by 31%) and the intensity of the thrombotic phenotype is diminished as compared with the $TM^{Pro/Pro}$ mice. For example, ambient fibrin levels in the lungs of $TM^{Pro/Pro}$ mice are increased 30-fold over wild-type mice, whereas fibrin levels in the lungs of the $TM^{-/-}$ chimeric mice are increased only 5-fold over wild-type mice, as determined by quantitative Western blotting. Also, $TM^{Pro/Pro}$ mice exposed to hypoxia (8% O_2 for 16 hours) show a 10-fold increase in fibrin over normoxic $TM^{Pro/Pro}$ mice as compared with only a 4-fold increase observed in the $TM^{-/-}$ chimeric mice (Fig 6). A second difference was noted when comparing the results of the immunocytochemical analysis of lung sections from the $TM^{Pro/Pro}$ mice, which revealed fibrin deposition in all segments of the vascular system (ie, microvessels, arteries, and veins), with the $TM^{-/-}$ chimeric mice, which revealed preferential fibrin deposition in larger vessels. TM mosaicism most likely contributes to this vascular bed-specific fibrin deposition observed only in the $TM^{-/-}$ chimeric mice. Finally, organ-specific differences in hemostatic function result from the distinct TM mutations. The $TM^{-/-}$ chimeric mice, like the $TM^{Pro/Pro}$ mice, display a dramatic increase in fibrin deposition in lung, but the $TM^{Pro/Pro}$ mice also display a marked fibrin deposition in the spleen and heart, whereas the $TM^{-/-}$ chimeric mice show an increased fibrin deposition in liver. Worth noting are the two different methods used to quantify cross-linked fibrin present in the vital organs of mice. Infusions of ^{125}I-labeled fibrinogen and measurements of cross-linked radiolabeled fibrin, used to examine $TM^{-/-}$ chimeric mice, reflect both fibrin deposition and dissolution over the 1-week time course. The quantitative Western blot for fibrin β-chains measures steady-state fibrin deposition. However, we do detect significant increased fibrin in the lungs of $TM^{-/-}$ chimeric mice using both techniques, suggesting that the organ-specific differences in TM function are not solely caused by methodology. A second possibility contributing to organ-specific differences in fibrin deposition between the two $TM^{-/-}$ mice is the age at which animals were analyzed. The $TM^{-/-}$ chimeric mice were examined both at 6 to 11 months and at 16 to 20 months, whereas the $TM^{Pro/Pro}$ mice were all less than 1 year old. However, knockout mice for the fibrinolytic proteins, urokinase, and tissue plasminogen activator also display organ-specific differences in fibrin deposition as measured by the quantitative Western blot technique,[26] indicating that organ-specific variations in endothelial cell hemostatic function exist and are not restricted to the TM/PC pathway.

The major similarity between the $TM^{-/-}$ chimeric and $TM^{Pro/Pro}$ mice is the increased fibrin deposition found in lungs. This may reflect the preferential expression of TM in normal mouse lung as compared with other highly vascularized organs[24] and suggests that in the lung the anticoagulant system may be more susceptible to alterations in the hemostatic mechanism and therefore more susceptible to thrombosis.

Comparison of the $TM^{-/-}$ chimeric mice with mice heterozygous for the TM mutation ($TM^{+/-}$) is also instructive. $TM^{+/-}$ mice have a 50% reduction in functional TM levels and protein C cofactor activity[12] as compared with the 31% reduction in cofactor activity in $TM^{-/-}$ chimeras. However, $TM^{+/-}$ mice show a uniform reduction in TM throughout the vasculature in contrast to the mosaic pattern found in $TM^{-/-}$ chimeras. We do not detect an increase in fibrin deposition/dissolution (as determined by ^{125}I-fibrinogen infusions) in $TM^{+/-}$ mice regardless of age (results not shown); this is in contrast to the 4-fold increase in fibrin deposition/dissolution in the TM chimeric mice (Fig 2). The $TM^{+/-}$ mice have a 3-fold increase in steady-state fibrin deposition[26] as compared with the 5-fold increase over wild-type levels observed in $TM^{-/-}$ chimeras. Therefore, the $TM^{+/-}$ mice have slightly lower levels of cofactor activity, but display a less pronounced phenotype. These results suggest that a focal TM deficiency is more likely to perturb hemostasis than a comparable but uniform TM deficiency. However, when these two mutant mice are exposed to hypoxia, it is the $TM^{+/-}$ mice that display a more striking phenotype. The $TM^{+/-}$ mice show a 10-fold increase in steady-state fibrin levels[26] as compared with a 4-fold increase in TM chimeras (Fig 6). These results suggest that exposure to a systemic thrombogenic challenge causes a more marked response in animals with a greater overall reduction in TM cofactor activity.

The third key element of the prothrombotic phenotype is age. The data support the existing hypothesis that age-related alterations in the coagulation mechanism predispose individuals harboring inherited, silent mutations in the anticoagulant mechanism to thrombosis. Indeed, the onset of thrombotic disease in humans has long been associated with advancing age. In addition to increased circulating levels of coagulation factors, the results of studies indicate significant increases in coagulation enzyme activation and fibrinolytic enzyme activity are age related.[32,33] This documentation of an age-dependent increase in coagulation system activity has led investigators to propose that an increase in circulating clotting factor activity may be a marker for predicting a ''prethrombotic state''. However, the results of a recent study have shown that in a group of healthy centenarians (25 individuals between the ages of 100 and 102 years), both coagulation system activation and fibrinolytic activity were markedly increased over younger healthy controls, yet these individuals were free of detectable thrombosis.[34] These results suggest that increased coagulation system activity associated with advanced age may be necessary but is not sufficient to induce a thrombotic state.

Age-dependent increases in coagulation system activity are not restricted to humans. Age-specific increases in the clotting factor, factor IX, have also been documented in C57BL/6 mice. Factor IX mRNA and cofactor activity are significantly upregulated in 28-month-old mice as compared with 2-month-old mice.[35] Thus, the combined effects of increased coagulation system activity in aging animals and the prolonged imbalance in the TM anticoagulant pathway are sufficient to induce the thrombotic state.

Finally, oxygen deprivation induces a thrombotic phenotype,

but the mechanisms by which hypoxia-induced pulmonary thrombosis occurs are unknown. Results of several recent studies in mice have defined events leading up to coagulation activation in response to hypoxia that may effect TM anticoagulant function. Within the first 2 to 4 hours after exposure to hypoxia and before the onset of fibrin deposition an increase in endothelial cell synthesized interleukin-6 is noted.[36] Increased cytokine levels are closely followed by the appearance of pulmonary mononuclear phagocytes expressing increased tissue factor and within 8 hours fibrin formation is detected.[37] Although the precise role the anticoagulant pathway plays in contributing to these early events has not been directly addressed, we noted that TM protein levels in lung remain unchanged after mice were exposed to hypoxia for 24 hours.[26] In the present study, we found that oxygen deprivation induces a thrombotic phenotype in both wild-type and in $TM^{-/-}$ mice as expected. However, the ambient levels of steady-state fibrin are increased fivefold to sixfold in the 6- to 11-month-old $TM^{-/-}$ mice as compared with wild-type mice, and fibrin formation in response to hypoxia is also increased fivefold to sixfold in $TM^{-/-}$ chimeras compared with wild-type mice. These data suggest that the TM pathway mediates the intensity of the thrombotic event and lends further support to the hypothesis that a threshold for anticoagulant function exists and is required for controlling hemostasis.

Extensive studies have shown the critical role that both heritable and acquired traits play in promoting intravascular thrombosis. Our data confirm and extend these previous findings and demonstrate that the extent of the TM deficiencies, the physical dimensions of the $TM^{-/-}$ regions, and the stresses associated with advancing age or environmental factors (ie, oxygen deprivation) accelerate the onset and severity of a thrombotic event. In conclusion, our findings support the novel concept that thrombosis resulting from a TM deficiency is a single-vessel, quantitative trait.

ACKNOWLEDGMENT

We thank Dr D.L. Rosene for the use of the BioQuant Imaging System and Dr E. Edelman for the use of an imaging work station.

REFERENCES

1. Comp PC, Jacocks RM, Ferrell GL, Esmon CT: Activation of protein C *in vivo*. J Clin Invest 70:127, 1982

2. Conard J, Bauer KA, Gruber A, Griffin JH, Schwarz HP, Horellou M-H, Samama MM, Rosenberg RD: Normalization of markers of coagulation activation with a purified protein C concentrat in adults with homozygous protein C deficiency. Blood 82:1159, 1993

3. Gladson CL, Scharrer I, Hach V, Beck KH, Griffin JH: The frequency of Type I heterozygous protein S and protein C deficiency in 141 unrelated young patients with venous thrombosis. Thromb Haemost 59:18, 1988

4. Esmon CT, Owen WG: Identification of an endothelial cell cofactor for thrombin-catalyzed activation of protein C. Proc Natl Acad Sci USA 78:2249, 1981

5. Jackman RW, Beeler DL, Fritze L, Soff G, Rosenberg RD: Human thrombomodulin gene is intron depleted: Nucleic acid sequence of the cDNA and gene predict protein structure and suggest sites of regulatory control. Proc Natl Acad Sci USA 84:6425, 1987

6. Boffa M-C, Burke B, Haudenschild CC: Preservation of thrombomodulin antigen on vascular and extravascular surfaces. J Histochem Cytochem 35:1267, 1987

7. Soff GA, Jackman RW, Rosenberg RD: Expression of thrombomodulin by smooth muscle cells in culture: Different effects of tumor necrosis factor and cyclic adenosine monophosphate on thrombomodulin expression by endothelial cells and smooth muscle cells in culture. Blood 77:515, 1991

8. Ford VA, Wilkinson JE, Kennel SJ: Thrombomodulin distribution during murine development. Roux's Arch Dev Biol 202:364, 1993

9. Imada M, Imada S, Iwasaki H, Kume A, Yamaguchi H, Moore EE: Fetomodulin: Marker surface protein of fetal development which is modulatable by cyclic AMP. Dev Biol 122:483, 1987

10. Imada S, Yamaguchi H, Imada M: Differential expression of fetomodulin and tissue plasminogen activator to characterize parietal endoderm differentiation of F9 embryonal carcinoma cells. Dev Biol 141:426, 1990

11. Weiler H, Aird W, Rayburn H, Husain M, Rosenberg RD: Developmentally regulated gene expression of thrombomodulin in postimplantation mouse embryos. Development 122:2271, 1996

12. Healy AM, Rayburn HB, Rosenberg RD, Weiler H: Absence of the blood clotting regulator thrombomodulin causes embryonic lethality in mice before development of a functional cardiovascular system. Proc Natl Acad Sci USA 92:850, 1995

13. Thomas KR, Capecchi MR: Site-directed mutagenesis by gene targeting in mouse embryo-derived stem cells. Cell 51:503, 1987

14. Mortensen RM, Conner DA, Chao S, Geisterfer AA, Seidman JG: Production of homozygous mutant ES cells with a single targeting construct. Mol Cell Biol 12:2391, 1992

15. Doetschman TC, Eistetter H, Katz M, Schmidt W, Kemler R: The in vitro development of blastocyst-derived embryonic stem cell lines: Formation of visceral yolk sac, blood islands and myocardium. J Embryo Exp Morph 87:27, 1985

16. Carrell N, McDonagh J: High resolution electrophoretic analysis of human fibrinogen and its crosslinked intermediates. Thromb Haemost 49:47, 1983

17. Mekori J, Dvorak HF, Galli S: ^{125}I-Fibrin deposition in contact sensitivity reactions in the mouse. Sensitivity of the assay for quantitating reactions after active or passive sensitization. J Immunol 136:2018, 1986

18. Bradley A: Production and analysis of chimaeras, in Robertson EJ (ed): Teratocarcinomas and Embryonic Stem Cells. Washington, DC, Oxford, 1987, p 147

19. Dvorak HF, Form DM, Manseau EJ, Smith BD: Pathogenesis of desmoplasia. J Natl Cancer Inst 73:1195, 1984

20. Hancock WW, Sayegh MH, Zheng XG, Peach R, Linsley PS, Turka LA: Costimulatory function and expression of CD 40-ligand, CD 80 and CD 86 in vascularized murine cardiac allograft rejection. Proc Natl Acad Sci USA 92:850, 1996

21. Risau W, Sariola H, Zerwes H-G, Sasse J, Ekblom P, Kemler R, Doetschman T: Vasculogenesis and angiogenesis in embryonic-stem-cell-derived embryoid bodies. Development 102:471, 1988

22. Wang R, Clark R, Bautch V: Embryonic stem cell-derived cystic embryoid bodies form vascular channels: An in vitro model of blood vessel development. Development 114:303, 1992

23. Bultman SJ, Michaud EJ, Woychik RP: Molecular characterization of the mouse agouti locus. Cell 71:1195, 1992

24. Ford VA, Stringer C, Kennel SJ: Thrombomodulin is preferentially expressed in Balb/c lung microvessels. Proc Natl Acad Sci USA 267:5446, 1992

25. Maruyama I, Bell CE, Majerus PW: Thrombomodulin is found on endothelium of arteries, veins, capillaries and lymphatics and on syncytiotrophoblast of human placenta. J Cell Biol 101:363, 1985

26. Weiler-Guetler H, Christie PD, Beeler DL, Healy AM, Hancock WW, Rayburn H, Edelberg JM, Rosenberg RD: A targeted point mutation in thrombomodulin generates viable mice with a prethrombotic state. J Clin Invest 101:1983, 1998

27. Miletich JP, Prescott SM, White R, Majerus PW, Bovill EG: Inherited predisposition to thrombosis. Cell 72:477, 1993

28. Ohlin AK, Marlar RA: The first mutation identified in the thrombomodulin gene in a 45-year-old man presenting with thromboembolic disease. Blood 85:330, 1995

29. Kumada T, Dittman WA, Majerus PW: A role for thrombomodulin in the pathogenesis of thrombin-induced thromboembolism in mice. Blood 71:728, 1987

30. Aird WC, Edelberg JM, Weiler-Guetler H, Simmons WW, Smith TW, Rosenberg RD: Vascular bed-specific expression of an endothelial cell gene is programmed by the tissue microenvironment. J Cell Biol 138:1117, 1997

31. Carmeliet P, Schoonjans L, Kieckens L, Ream B, Degen J, Bronson R, De Vos R, van den Oord J, Collen D, Mulligan RC: Physiological consequences of loss of plasminogen activator gene function in mice. Nature 368:419, 1994

32. Bauer KA, Weiss LM, Sparrow D, Vokonas PS, Rosenberg RD: Aging-associated changes in indices of thrombin generation and portein C activation in humans. J Clin Invest 80:1527, 1987

33. Kario K, Matsuo T: Lipid-related abnormalities in the elderly: Imbalance between coagulation and fibrinolysis. Atherosclerosis 103: 131, 1993

34. Mari D, Mannucci PM, Coppola R, Bottasso B, Bauer KA, Rosenberg RD: Hypercoagulability in centenarians: The paradox of successful aging. Blood 85:3144, 1995

35. Boland EJ, Liu YC, Walter CA, Herbert DC, Weaker FJ, Odom MW, Jagadeeswaran P: Age-specific regulation of clotting factor IX gene expression in normal and transgenic mice. Blood 86:2198, 1995

36. Yan SF, Tritto I, Pinsky D, Liao H, Huang J, Fuller G, Brett J, May L, Stern D: Induction of interleukin-6 (IL-6) by hypoxia in vascular cells. J Biol Chem 270:11463, 1995

37. Lawson CA, Yan SD, Yan SF, Liao H, Zhou YS, Sobel J, Kisiel W, Stern DM: Monocytes and tissue factor promote thrombosis in a murine model of oxygen deprivation. J Clin Invest 99:1729, 1997